Biomarkers, 2012; 17(1): 48–55

ISSN 1354-750X print/ISSN 1366-5804 online
DOI: 10.3109/1354750X.2011.637180

informa
healthcare

RESEARCH ARTICLE

Serum metabonomics study of adenine-induced chronic renal failure in rats by ultra performance liquid chromatography coupled with quadrupole time-of-flight mass spectrometry

Ying-Yong Zhao[1], Xian-Long Cheng[2], Feng Wei[2], Xin-Yue Xiao[2], Wen-Ji Sun[1], Yongmin Zhang[3], and Rui-Chao Lin[2]

[1]*Department of Traditional Chinese Medicine, the College of Life Sciences, Northwest University, Shaanxi, China,*
[2]*National Institutes for Food and Drug Control, State Food and Drug Administration, Beijing, China, and*
[3]*Université Pierre & Marie Curie-Paris 6, Institut Parisien de Chimie Moléculaire, Paris, France*

Abstract

An ultra performance liquid chromatography coupled with quadrupole time-of-flight mass spectrometry (UPLC Q-TOF MS) metabonomics approach was employed to study the serum metabolic profiling of adenine-induced chronic renal failure (CRF) rats. Acquired data were subjected to principal component analysis (PCA) for differentiating the CRF and the normal control groups. Potential biomarkers were screened by using S-plot and were identified by the accurate mass, isotopic pattern and MS/MS fragments information obtained from UPLC Q-TOF MS analysis. Significant differences in the serum level of creatinine, amino acids and LysoPCs were observed, indicating the perturbations of amino acid metabolism and phospholipid metabolism in adenine-induced CRF rats. This research proved that metabonomics is a promising tool for disease research.

Keywords: Chronic renal failure, metabonomics, serum, rats, UPLC Q-TOF MS

Introduction

Chronic renal failure (CRF) is one of the most important public health problems, with increasing rates of incidence and prevalence (Collins et al., 2005). The early appearance of renal hypertrophy, the progressive accumulation of extracellular matrix in the glomerulus and tubulointerstitium, and consequently, glomerulosclerosis, tubulointerstitial fibrosis and tubular atrophy are the major morphological features of CRF (Wolf, 2006). The various end-stage renal diseases can lead to chronic renal failure. However, their histopathological appearance is commonly renal interstitial fibrosis, which represents an irreversible process and signifies a poor prognosis (Yu, 2003; Nangaku, 2004). CRF is a serious clinical symptom, and it is the end result of all kinds of chronic kidney diseases. Their important pathophysiological and clinical characters are the decrease of renal function, i.e. accumulation of metabolites and toxins, unbalance of water, electrolytes and acid–base and some abnormalities of endocrine function. As the mechanism of chronic renal failure is not yet clear, chronic renal failure can be not treated by effective methods. The fact that it finally resulted in CRF is doubtless (Coresh et al., 2003; Locatelli et al., 2006; Zoccali, 2006).

Metabonomics, which has been defined as "the quantitative measurement of the dynamic multi-parametric metabolic response of living organisms to pathophysiological stimulation or genetic modifications" (Nicholson et al., 1999), is emerging as a systematic approach to deal with changes in small molecular metabolites (MW<1000Da) following toxic exposure, disease or variation in genetic function. By building up spectra library from hepatotoxicity, nephrotoxicity and cancer patients, metabonomics may act as a preclinical or clinical screening tool for potential patients. As a powerful analytical platform, recently, the application of metabonomics has

Address for Correspondence: Ying-Yong Zhao, Department of Traditional Chinese Medicine, the College of Life Sciences, Northwest University, No.229 Taibai North Road, Xi'an, Shaanxi 710069, China. Tel: +86 29 88304569. Fax: +86 29 88304368. E-mail: zyy@nwu.edu.cn; zhaoyybr@163.com

(Received 06 September 2011; revised 14 October 2011; accepted 29 October 2011)

dramatically increased in the fields of pharmaceutical discovery and development (Lindon et al., 2006; Lindon et al., 2007; Robertson et al., 2007), evaluation of drug efficacy and toxicity (Griffin et al., 2004; Chen et al., 2006), therapy and novel potential biomarker discovery (Li et al., 2007; Kellert et a*l*., 2008).

There is a great interest in the development of many analytical techniques and strategies for biomarker discovery (Johnson and Plumb 2005; Yin et al., 2006; Dunn et al., 2007). Nuclear magnetic resonance (NMR) spectroscopy is an efficient and nondestructive tool for generating data of metabolites in biofluids or tissues (Keun et al., 2002; Khandelwal et al., 2004; Constantinou et al., 2005). Analytical methods based on HPLC/MS and GC/MS have been more and more used in metabonomics (Kuhara, 2005; Yang et al., 2006). In order to obtain better quality and higher throughput in complex mixture analysis, the new analytical technique of ultra-performance liquid chromatography (UPLC) has been developed (Plumb et al., 2005; Wilson et al., 2005; Desmond and Russell, 2006). UPLC Q-TOF MS uses small particle size packings in the column to provide better chromatographic resolution. So it is considered as a powerful metabonomics tool. UPLC Q-TOF MS has been used to study the serum metabolites of the patients with CRF and it is suitable for the analysis of in vivo (Jia et al., 2008). However, A better understanding of the metabonomics of an animal model as well as the structure of its potential biomarkers are important for predicting the therapeutic outcome of the drug in pre-clinical or clinical trials and explain toxicity. Animal models are widely used for the drug in pre-clinical studies. Serum is the most widely used specimen for exploring the systematic alteration of metabolite in human or animal because the collection and treatment of these samples are relatively easy. In this article, Adenine-induced CRF model rats were established by treating the male Sprague-Dawley (SD) rats with adenine (Yokozawa et al., 1986). Corresponding serum samples were collected from the adenine-induced CRF and normal control rats for the metabonomics analysis by using UPLC Q-TOF MS. Principal component analysis (PCA) was performed for investigating the metabolic changes of adenine-induced CRF rats, and the potential biomarkers were identified accordingly.

Experimental

Chemicals and reagents

Adenine (batch No.: A8626, Purity 99.0%) was purchased from Sigma Chemical Co., Ltd (St. Louis, MO, USA). Creatinine (batch No.: 100877-200901, Purity 99.8%) was obtained from the National Institutes for Food and Drug Control (Beijing, China). L-tryptophan (batch No.: TB1991-25g, Purity 99.0%) was purchased from Amresco Company (Amresco Inc., USA). HPLC-grade methanol and acetonitrile was purchased from Baker Company (Baker Inc., USA). Ultra high purity water was prepared by a Millipore-Q SAS 67120MOLSHEIM (France). Other chemicals were of analytical grade and their purity was above 99.5%.

Animals and sample collection

The study was conducted in accordance with the Regulations of Experimental Animal Administration issued by the State Committee of Science and Technology of People's Republic of China. All procedures and the care of the rats were in accordance with institutional guidelines for animal use in research. Male Sprague-Dawley (SD) rats were obtained from the Central Animal Breeding House of Xi'an Jiaotong University (Xi'an, China). They were maintained at a constant humidity (ca. 60%) and temperature (ca. 23°C) with a light/dark cycle of 12 h.

Male rats underwent an adaptation period of several days, during which they were fed a commercial feed. The rats weighing 190–210 g were divided into 2 groups after measuring of body weight. Group 2 then were given 200 mg/kg body weight of adenine dissolved with 1% (w/v) gum acacia solution (by gastric gavage, instead of adenine added in food) (Yokozawa et al., 1986), which produced experimental renal failure in the animal for three weeks. Group 1 was similarly given with an equal volume of gum acacia solution. Body weight was measured daily for all rats. Rats were anesthetized with 10% urethane, and blood samples containing EDTA anticoagulant were obtained by carotid artery cannula. Blood was centrifuged at 3000 rpm for 10 min and the supernatant was collected and stored at –80°C

Sample preparation

Prior to analysis, the serum samples were thawed at room temperature. Acetonitrile (400 μL) was added to serum (200 μL) and vortex-mixed vigorously for 3 min. The mixture was settled at room temperature for 10 min, and then centrifuged at 13000×*g* for 10 min at 4°C. The supernatant (400 μL) were pipetted out and lyophilized.

Chromatographic separation

The UPLC analysis was performed with a Waters Acquity™ Ultra Performance LC system (Waters, USA) equipped with a Waters Xevo™ G2 QTof MS (Waters MS Technologies, Manchester, UK). Chromatographic separation was carried out at 45°C on an ACQUITY UPLC BEH C18 column (2.1 × 100 mm, 1.7 μm, UK). The mobile phase consisted of water (A) and acetonitrile (B), each containing 0.1 % formic acid. The optimized UPLC elution conditions were: 0–0.5 min, 1% B; 0.5–3.5 min, 1–35% B; 3.5–7.0 min, 35–99% B; 7.0–8.0 min, 99% B and 8.0–10.0 min, 99.0–1.0% B. The flow rate was 0.45 mL/min. The autosampler was maintained at 4°C. The lyophilized serum samples were dissolved in 100 μL of distilled acetonitrile/water (4:1). Every 2 μL sample solution was injected for each run.

Mass spectrometry

Mass spectrometry was performed on a Xevo™ G2 QTof (Waters MS Technologies, Manchester, UK), a

quadrupole and orthogonal acceleration time-of-flight tandem mass spectrometer. The scan range was from 50 to 1200 *m/z*. For both positive and negative electrospray modes, the capillary and cone voltage were set at 3.0 kV and 30 V, respectively. The desolvation gas was set to 800 L/h at a temperature of 450°C; the cone gas was set to 20 L/h and the source temperature was set to 150°C. The mass spectrometry was operated in W optics mode with 12,000 resolution using dynamic range extension (DRE). The data acquisition rate was set to 0.1 s, with a 0.1 s interscan delay. All analyses were acquired using the lockspray to ensure accuracy and reproducibility. Leucine–enkephalin was used as the lockmass at a concentration of 300 ng/mL and flow rate of 5 μL/min. Data were collected in continuum mode, the lockspray frequency was set at 10 s, and data were averaged over 10 scans. All the acquisition and analysis of data were controlled by Waters MassLynx v4.1 software.

Data analysis

The raw data were analyzed using the MarkerLynx XS software (Waters Corp). This software allowed deconvolution, alignment and data reduction to give a list of mass and retention time pairs with corresponding intensities for all the detected peaks from each data file in the data set. The main parameters were set as follows: retention time range 0–8.5 min, mass range 100–1000 amu, mass tolerance 0.02, minimum intensity 5%, mass window 0.05, retention time window 0.20, and noise elimination level 6. The resulting data were analyzed by PCA and partial least squares-discriminate analysis (PLS-DA) using SIMCA-P 11.0 (Umetrics AB, Umeå, Sweden). The statistical analysis was performed by SPSS 11.0 (SPSS Inc., Chicago, USA). For the identification of potential markers, the following databases have been used: HMDB (http://www.hmdb.ca/), METLIN (http://metlin.scripps.edu/), Massbank (http://www.massbank.jp), PubChem (http://ncbi.nlm.nih.gov/) and KEGG (http://www.genome.jp/kegg/).

Results and discussion

Pathological characteristics of adenine-induced CRF rats

Figure 1 shows the body weight in the normal control and adenine-induced CRF rats over the 3-week study period. The body weight of adenine-induced rats increased at a slower manner when compared with that of the normal control ones (Figure 1). For the fact that both groups of rats were allowed free access to water and food, the result demonstrated that adenine induced a decrease in growth rate in rats. Abnormal reabsorption ability of renal tubules could be the causes for the decrease in growth in the adenine-induced rats. As shown in Table 1, the normal levels of Scr and BUN of rats are 33.5 μmol/L and 6.8 mmol/L (n = 6), respectively. The Scr level in only adenine-induced CRF rats markedly increased beyond the normal level. Similarly, the BUN level in adenine-induced CRF rats increased to ca. 28.6 mmol/L. Figure 2

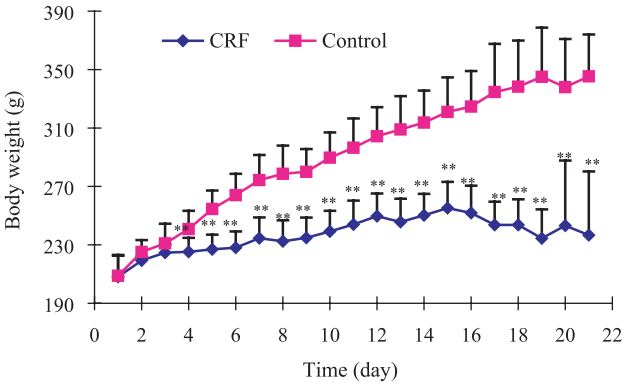

Figure 1. Body weight of the normal control and adenine-induced CRF rats. *$P<0.05$, **$P<0.01$ (compared with health control group).

Table 1. SUN and serum creatinine levels in normal control and adenine-induced CRF rats.

	Normal control rats	Adenine-induced rats
SUN (mmol/l)	6.8 ± 1.7	36.1 ± 5.5**
Scr (μmol/l)	34.6 ± 2.6	124.2 ± 14.9**

**Significantly different from the value of normal control rats ($p<0.001$).

shows histologic findings by hematoxylin–eosin (HE) staining of transverse kidney sections in the normal control rats (Figure 2A), adenine-induced rats in 10-day study period (Figure 2B), and adenine-induced rats in 20-day study period (Figure 2C). There was formation of foreign body granuloma in the renal tubules and interstitium, and marked fibrosis leading in some extreme cases to contracted kidney. These results demonstrate that the rat model exhibited typical pathologic features associated with chronic renal failure.

Sample preparation and UPLC-MS analysis

The complexity of the serum sample makes the separation very difficult, consequently results in severe ion suppression. UPLC employs smaller stationary phase particle size column, generating high efficiency to the separation, which concurrently increases resolution and sensitivity. Here, we applied UPLC to obtain the metabolic profiles of the serum of normal control and adenine-induced CRF rats in the positive ESI modes. A typical base peak intensity (BPI) chromatograms of the serum of adenine-induced CRF rat is shown in Figure 3. The average peak width for this separation is 4 s at peak base, which generated a series of peaks with retention time and *m/z* pairs (t_{R}_*m/z* pair) as variables. To minimize thermal degradation of the metabolites while waiting to be analyzed, the auto-sampler compartment was set at 4°C throughout the analysis.

High reproducibility is crucial for any analytical protocols, especially for metabonomics study which requires handling many samples. Reproducibility of the chromatography and MS was determined from ten replicated analyses of the same serum sample. The variations of retention times and *m/z* values of randomly selected

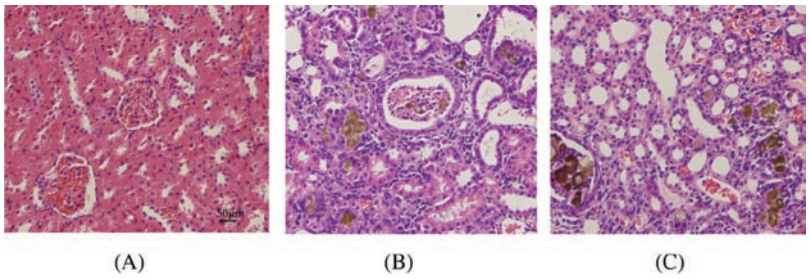

Figure 2. Histologic findings by HE-staining of transverse kidney sections in the normal control rats (A), adenine-induced rats in 10-day study period (B), and adenine-induced rats in 20-day study period (C). Scale bar, 50 μm.

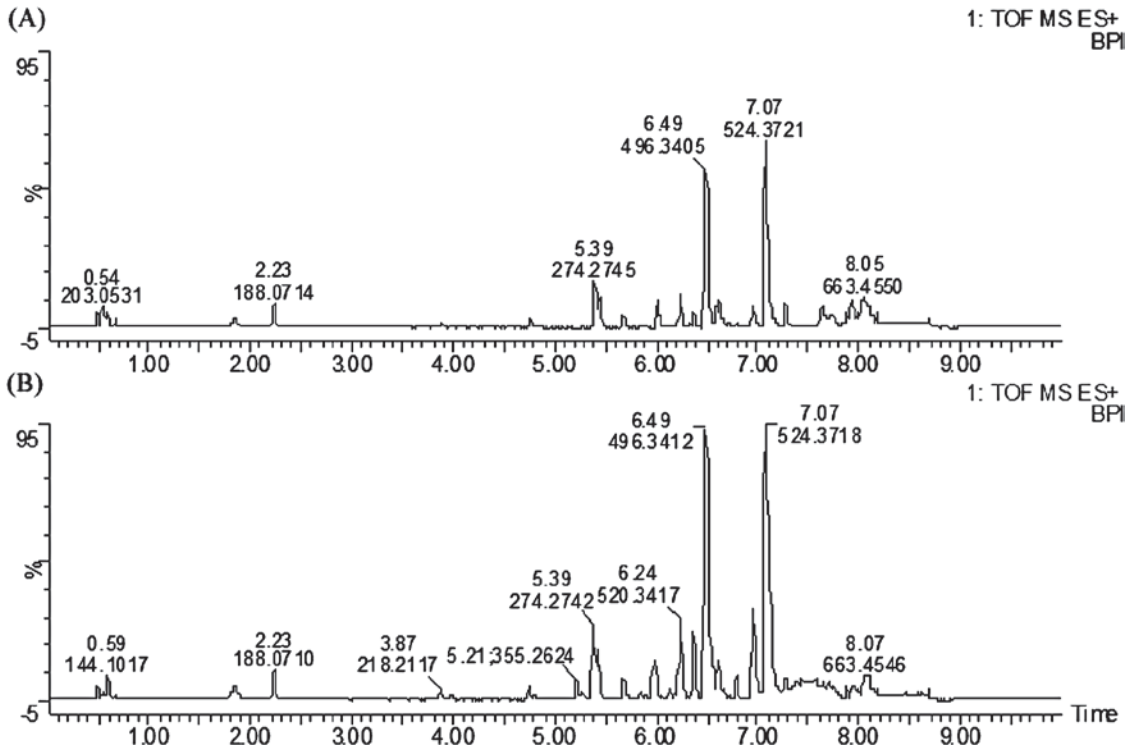

Figure 3. Base peak intensity (BPI) chromatograms obtained from the positive ion UPLC-MS analyses of normal control (A) and adenine-induced CRF (B) rats.

peaks in positive ESI modes were less than 0.04 min and 8 mDa, respectively, and the relative standard deviations of retention time and peak area are below 0.72 and 3.8%, respectively. These results demonstrated the excellent stability and reproducibility of chromatographic separation and mass measurement during the whole sequence.

Multivariate data analysis of UPLC Q-TOF MS data

PCA is an unsupervised multivariate data analysis method and it gives the comprehensive view of the clustering trend for the multidimensional data. According to UPLC–MS data, 4340 peaks were detected and processed by MarkerLynx XS using the same acquiring method. In order to gain an overview of the rat serum metabolic profiling, PCA was used in the subsequent UPLC Q-TOF MS data analysis. The parameter R^2X shows the fit proportion of variance of the CRF model and indicates goodness of fit. Figure 4A and B shows the PCA score plot and S-plot of the adenine-induced CRF rats and normal controls based on the serum metabolic profiles. In the serum PCA score plot, the adenine-induced CRF and normal control groups were separated clearly. The two components explained 71.2% of the total variances. The results from the unsupervised analysis of PCA showed significant metabolic changes occurring in the adenine-induced CRF rats.

Identification of potential biomarkers

In today's metabonomics research, the biggest challenge is the identification of potential biomarker obtained from comparative samples, particularly when they are novel and published work on the compound class is unavailable or prior information is lacking otherwise. Variables were selected according to the VIP (Variable Importance in the Projection) values, which reflect the influence of each metabolite in the two groups. To discover potential biomarkers among the thousands of variables, the

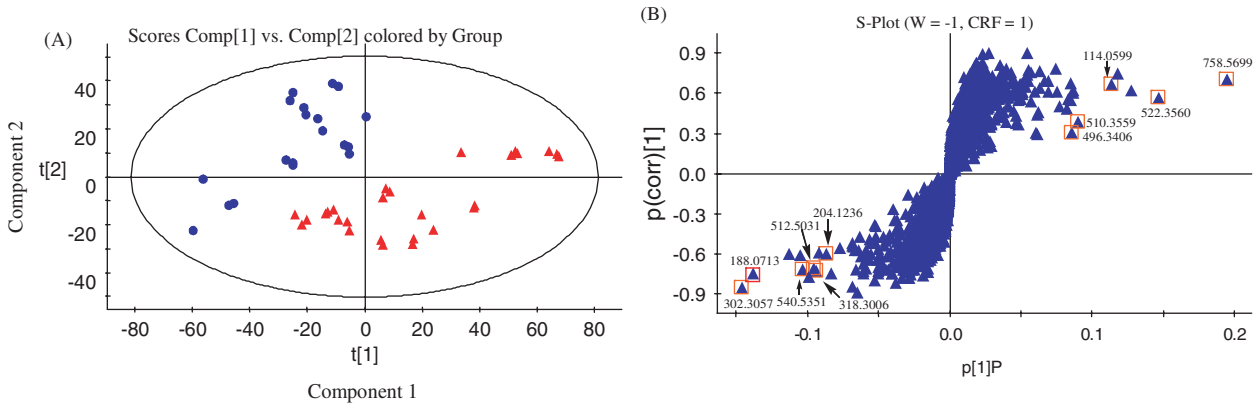

Figure 4. (A) PCA score plot based on the serum metabolic profiling of the adenine-induced CRF (●) and normal control (▲) rats; (B) S-plot used in our biomarkers selection. The variables marked (□) are the metabolites selected as potential biomarkers.

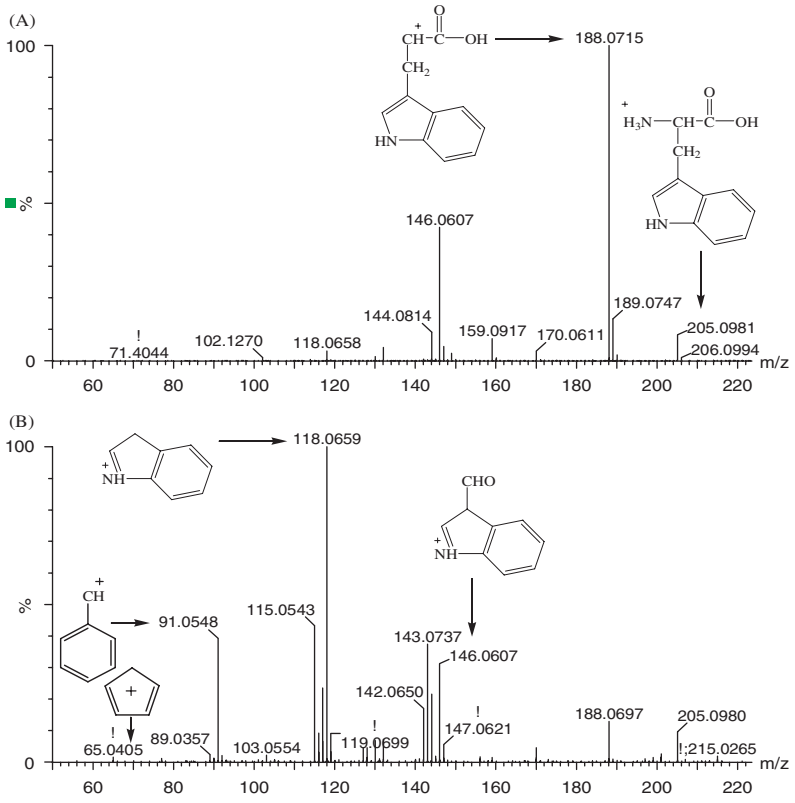

Figure 5. Mass spectra of biomarker at (A) *m/z* 188.0713 and (B) product ion scan spectrum of the biomarker in positive ion mode.

20 potential biomarkers with the highest VIP values were selected for further analysis. The S-plot (shown in Figure 4B) is a visual method that can be used for selection of biomarkers. Variables that are farthest from the origin in the S-plot are selected as potential biomarkers. In our study, biomarkers were tentatively identified based on accurate mass measurements via UPLC Q–TOF MS, comparison of theoretical to observed isotopic patterns, MS/MS experiments, or comparison to authentic standards. Here, we take *m/z* 188.0715 as an example to illustrate the identification process. Besides the base peak ion at *m/z* 188.0715, the ion at *m/z* 205.0981 was found in positive ion spectrum (Figure 5A). Thus, we infer that the quasi-molecular ion is *m/z* 205.09 ($[M+H]^+$) and the ion at *m/z* 188.0715 is the fragment ion ($[M–NH_3]^+$). With different collision energies, the corresponding MS^E information was obtained (Figure 5B). In positive ionisation mode, the detected ions included 146.0607, 118.0659, 91.0548 and 65.0405 were found (Figure 5B). The ion at *m/z* 91.0548 and 65.0405 are the fragment ion of benzyl and phenyl group, respectively. To define its structure, some databases like MASSBANK (http://www.massbank.jp) and HMDB (http://www.hmdb.ca/) were searched with the molecular weight 205.0981Da, then some compounds without one phenyl group were removed from the candidate list. Furthermore, under the

Table 2. The most prominent metabolites discriminated of adenine-induced CRF rats compared to normal control rats.

t_R (min)	*m/z*	Element composition	Identification result	*P* value	Trend
7.71	758.5699	$C_{34}H_{69}NO_3$	PC(16:0/18:2)	<0.001	↑
6.61	522.3560	$C_{16}H_{30}O_3$	LysoPC(18:1)	<0.001	↑
5.80	302.3057	$C_{18}H_{39}NO_2$	Dihydrosphingosine	<0.001	↓
2.22	188.0713	$C_{11}H_{12}N_2O_2$	Tryptophan	<0.001	↓
5.28	274.2745	-	Unknown	<0.001	↓
5.21	355.2634	-	Unknown	<0.001	↑
0.57	114.0599	$C_4H_7N_3O$	Creatinine	<0.001	↑
7.48	540.5351	$C_{29}H_{49}O_{12}P$	Ceramides (18:0/16:0)	<0.001	↓
7.35	512.5031	$C_{32}H_{65}NO_3$	Ceramides (18:0/14:0)	<0.001	↓
0.64	204.1236	$C_9H_{17}NO_4$	L-Acetylcarnitine	<0.001	↓
6.79	510.3559	$C_{10}H_{13}NO_4$	LysoPC(17:0)	<0.001	↑
6.47	496.3406	$C_4H_7N_3O$	LysoPC (16:0)	<0.001	↑
5.31	318.3006	$C_{18}H_{39}NO_3$	Phytosphingosine	<0.001	↓

[a]*P* value of independent *t* test.
The levels of potential biomarkers were labeled with (↓) down-regulated and (↑) up-regulated.

same liquid chromatography condition, the sample was injected to ESI–Q–TOF MS, at the same retention time, accurate molecular weight *m/z* 205.0978 was found and it was the only peak in the extracted ion chromatogram (*m/z* 205.09). Finally, it was tentatively identified as tryptophan. By using the same method described above, eleven potential biomarkers were identified. Table 2 displays the identification results of potential biomarkers showing concentration difference between the adenine-induced CRF and normal control rats based on serum metabolic profiling (ESI^+ mode).

Study of metabolic changes and biochemical interpretation in adenine-induced CRF rats

Under certain situations, the differences of some metabolic pathways between human and animals make it difficult to predict a toxicology effect in human beings with metabonomics studies using animal model. Therefore, it is tremendously important for metabonomics investigation to choose suitable experimental animals which are close to human in genotype, phenotype and metabolic type. Adenine-rich diets increase serum uric acid, creatinine and SUN by decreasing the urinary excretion of these substances (Yokozawa et al., 1986). Yokzawa et al. reported a new animal model of CRF induced by an adenine-rich diet. Adenine produces metabolic abnormalities resembling chronic renal insufficiency in humans (Yokozawa et al., 1986). According to Yokzawa et al., excretion of nitrogen compounds is suppressed by renal tubular occlusion due to 2,8-dihydroxyadenine. This, in turn, leads to accumulation of urea nitrogen and creatinine in the blood, with a resultant increase of various guanidine compounds (Yokozawa et al., 1986). These metabolic changes, which are widespread in human and other mammalian species including rodents, have been successfully applied in many medical studies to demonstrate drug's toxicological or pharmacological action. However, for the future metabonomics study on certain

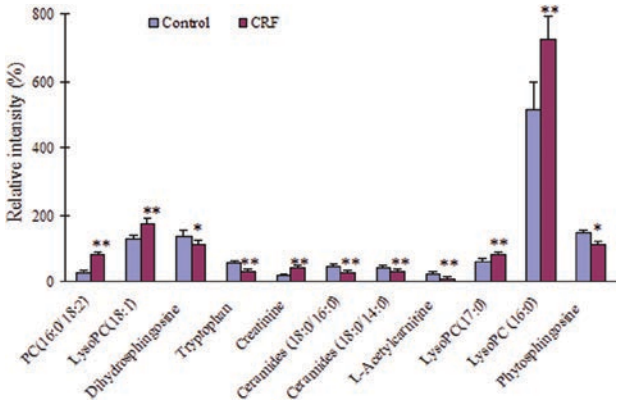

Figure 6. Comparison of the relative intensity of putative potential biomarkers in the normal control and adenine-induced CRF rats.

complicated physiological and pathological mechanisms, experimental animals having closer genetic relationship with humans such as primates and humanized animals should be chosen.

To investigate the change of the potential biomarkers in the body fluids of adenine-induced CRF rats, we compared the relative intensity of putative potential biomarkers in serum (Figure 6) in the normal control and adenine-induced CRF rats. In the plasma of atherosclerosis rats, concentrations of PC(16:0/18:2), lysoPC(18:1), creatinine, lysoPC(17:0) and lysoPC (16:0) were all up-regulated, but dihydrosphingosine, tryptophan, ceramides (18:0/16:0), ceramides (18:0/14:0), L-acetylcarnitine and phytosphingosine were down-regulated. These metabolites mentioned above might play important roles in the metabolic changes of adenine-induced CRF rats.

Creatinine is a potential biomarker for the separation of adenine-induced CRF group. Increase of creatinine was observed in serum metabolite profiles of the adenine-induced CRF group compared with the control group. Creatinine is the end product of protein metabolism in animal or human body. It is an important biomarker to

evaluate renal function. It is reported that animal models with adenine-induced CRF is associated with progressive renal disturbances (Yokozawa et al., 1986).

Amino acids serve as substrates for protein synthesis, metabolic energy, or gluconeogenesis and ketogenesis. Tryptophan is an essential amino acid which cannot be synthesized by the body. When the CRF model was made, tryptophan was significantly decreased in the model group compared with that in the control group. The metabolism pathway of tryptophan may be partly disturbed. Change of the amino acid in adenine-induced CRF rats may indicate an alteration of the balance between nutrition intake and consumption. The increase of energy and protein expenditure could be the main reasons for the decrease of tryptophan. Based on our study, compared with the normal control group, tryptophan decreased remarkably in adenine-induced CRF rats, which may showed that renal injury progress is involved in amino acid metabolism (Yokozawa et al., 1986).

It is becoming increasingly clear that lipids play key roles in regulating cellular function. Phospholipids have the important roles in signal processing and as the precursors of many other biologically active molecules (Lemmon, 2003; Dolones et al., 2005; Jackson et al., 2005; Wenk, 2005). Dihydrosphingosine and phytosphingosine are classified into sphingolipids, and play important roles in the sphingolipids biosynthesis and metabolism. The application of UPLC Q-TOF MS coupled with PCA makes it possible to show the fact that the phospholipids molecules of experimental adenine-induced CRF rats are obviously different from those of the normal control rat. In our study, an obvious decrease of dihydrosphingosine and phytosphingosine in CRF rats was observed, consequently resulting in the decrease of ceramide content. At present, the relationship of the change of phospholipids and CRF is not very clear yet. The possible mechanism is that phosphatidylinositol is hydrolyzed by activating phosphatidylinositol-specific phospholipase C, meanwhile, it comes to be two second messengers, insositol (1,4,5)– trisphosphate and diacylglycerol (Rhee, 2001), which take part in signal transfer system by two independent and interaction ways. IP3 induces sarcoplasmic reticulum to release Ca^{+} and increases the concentration of Ca^{+} (Cantley, 2002). Protein kinase C is activated by the participation of phosphatidylserine, Ca^{+} and diacylglycerol. The intracellular protein kinase C signal transfer system is activated, which takes part in a series of physiological and physiochemical procedures: (1) The activation of protein kinase C channel causes extracellular matrix accumulate and make vascular basement membrane to thicken (Fukui et al., 1992). (2) Vascular permeability is increased: Protein kinase C increasing the permeability of epithelial cell is realized by phosphorylation changing the structure and function of epithelial cell, and weaken the connection between cells and between cell and matrix, thus, the space between epithelial cells is increased (Lynch et al., 1990). Epithelial cell and basement membrane constitute glomerular capillary barrier. As a result of PKC activation, the glomerular capillary barrier is injured, which results in proteinuria. (3) Na^{+}-K^{+}-ATPase activation is decreased: Na^{+}-K^{+}-ATPase is the substratum of protein kinase C activation. After protein kinase C is activated, the activation of Na^{+}-K^{+}-ATPase is decreased. Therefore, the intracellular osmotic pressure is affected, and consequent the integrality of cell is also affected.

The finding of these new biomarkers not only showed that the disturbance of amino acid metabolism and phospholipids metabolism was of great importance for the CRF rats, but also indicated that nutritional treatment was crucial for the CRF disease. However, some potential biomarkers were unable to be identified with current methods due to the restriction of metabolite databases and the shortage of standard compounds. Further research of the physiological change and mechanism of adenine-induced CRF rats requires more animal experiments and powerful analytical strategy, especially structural identification technique.

Conclusions

A metabonomics method based on UPLC Q-TOF MS and amultivariate statistical technique has been successfully used to study adenine-induced CRF. The PCA scores plot showed the complete distinction of CRF groups and normal control group. Furthermore, significant differences in the serum level of creatinine, amino acids and LysoPCs were observed, compared with those of the normal controls. These results indicated the perturbations of amino acid metabolism and phospholipids metabolism of adenine-induced CRF. The study demonstrates that the metabonomics based on UPLC Q-TOF MS could reflect the balance of homeostasis and metabolism of nourishment, and is a promising tool to find and identify potential biomarkers.

Acknowledgements

The authors wish to thank Xu Bai for his expert technical assistance from Waters Technology (Shanghai) Co., Ltd.

Declaration of interest

This study was supported in part by grants from the National Scientific Foundation of China (No. 81001622), project of "As a Major New Drug to Create a Major National Science and Technology Special" (No. 2011ZX09401-308-34) from Ministry of Science and Technology of the People's Republic of China and Scientific Research Program Funded by Shaanxi Provincial Education Department (No. 11JK0678).

References

Cantley LC. (2002). The phosphoinositide 3-kinase pathway. *Science* 296:1655–1657.

Chen M, Su M, Zhao L, Jiang J, Liu P, Cheng J, Lai Y, Liu Y, Jia W. (2006). Metabonomic study of aristolochic acid-induced nephrotoxicity in rats. *J Proteome Res* 5:995–1002.

Collins AJ, Kasiske B, Herzog C, Chavers B, Foley R, Gilbertson D, Grimm R, Liu J, Louis T, Manning W, Matas A, McBean M, Murray A, St Peter W, Xue J, Fan Q, Guo H, Li S, Li S, Roberts T, Snyder J, Solid C, Wang C, Weinhandl E, Arko C, Chen SC, Dalleska F, Daniels F, Dunning S, Ebben J, Frazier E, Johnson R, Sheets D, Forrest B, Berrini D, Constantini E, Everson S, Frederick P, Eggers P, Agodoa L; United States Renal Data System. (2005). Excerpts from the United States Renal Data System 2004 annual data report: Atlas of end-stage renal disease in the United States. *Am J Kidney Dis* 45:A5–7, S1.

Constantinou MA, Papakonstantinou E and Spraul M. (2005). ^{1}H NMR-based metabonomics for the diagnosis of inborn errors of metabolism in urine. *Anal Chim Acta* 511:303–312.

Coresh J, Astor BC, Greene T, Eknoyan G, Levey AS. (2003). Prevalence of chronic kidney disease and decreased kidney function in the adult US population: Third National Health and Nutrition Examination Survey. *Am J Kidney Dis* 41:1–12.

Desmond O, and Russell M-S. (2006). High-throughput bioanalysis with simultaneous acquisition of metabolic route data using ultra performance liquid chromatography coupled with time-of-flight mass spectrometry. *Anal Bioanal Chem* 385:114–121.

Downes CP, Gray A, Lucocq JM. (2005). Probing phosphoinositide functions in signaling and membrane trafficking. *Trends Cell Biol* 15:259–268.

Dunn WB, Broadhurst DI, Deepak SM, Buch MH, McDowell G, Spasic I, Ellis DI, Brooks N, Kell DB and Neyses L. (2007). Serum metabolomics reveals many novel metabolic markers of heart failure, including pseudouridine and 2-oxoglutarate. *Metabolomics* 3:413–426.

Fukui M, Nakamura T, Ebihara I, Shirato I, Tomino Y, Koide H. (1992). ECM gene expression and its modulation by insulin in diabetic rats. *Diabetes* 41:1520–1527.

Griffin JL, Bollard ME. (2004). Metabonomics: Its potential as a tool in toxicology for safety assessment and data integration. *Curr Drug Metab* 5:389–398.

Jackson SN, Wang HY, Woods AS, Ugarov M, Egan T, Schultz JA. (2005). Direct tissue analysis of phospholipids in rat brain using MALDI-TOFMS and MALDI-ion mobility-TOFMS. *J Am Soc Mass Spectrom* 16:133–138.

Jia LW, Chen J, Yin PY, Lu X and Xu GW. (2008). Serum metabonomics study of chronic renal failure by ultra performance liquid chromatography coupled with Q-TOF mass spectrometry. *Metabolomics* 4:183–189.

Johnson KA, Plumb R. (2005). Investigating the human metabolism of acetaminophen using UPLC and exact mass oa-TOF MS. *J Pharm Biomed Anal* 39:805–810.

Kellert M, Wagner S, Lutz U, Lutz WK. (2008). Biomarkers of furan exposure by metabolic profiling of rat urine with liquid chromatography-tandem mass spectrometry and principal component analysis. *Chem Res Toxicol* 21:761–768.

Keun HC, Beckonert O, Griffin JL, Richter C, Moskau D, Lindon JC, Nicholson JK. (2002). Cryogenic probe 13C NMR spectroscopy of urine for metabonomic studies. *Anal Chem* 74:4588–4593.

Khandelwal P, Beyer CE, Lin Q, McGonigle P, Schechter LE, Bach AC 2nd. (2004). Nanoprobe NMR spectroscopy and *in vivo* microdialysis: New analytical methods to study brain neurochemistry. *J Neurosci Methods* 133:181–189.

Kuhara T. (2005). Gas chromatographic-mass spectrometric urinary metabolome analysis to study mutations of inborn errors of metabolism. *Mass Spectrom Rev* 24:814–827.

Lemmon MA. (2003). Phosphoinositide recognition domains. *Traffic* 4:201–213.

Li F, Lu X, Liu H, Liu M, Xiong Z. (2007). A pharmaco-metabonomic study on the therapeutic basis and metabolic effects of Epimedium brevicornum Maxim. on hydrocortisone-induced rat using UPLC-MS. *Biomed Chromatogr* 21:397–405.

Lindon JC, Holmes E, Nicholson JK. (2006). Metabonomics techniques and applications to pharmaceutical research & development. *Pharm Res* 23:1075–1088.

Lindon JC, Holmes E, Nicholson JK. (2007). Metabonomics in pharmaceutical R&D. *FEBS J* 274:1140–1151.

Locatelli F, Del Vecchio L, Pozzoni P, Manzoni C. (2006). Nephrology: Main advances in the last 40 years. *J Nephrol* 19:6–11.

Lynch JJ, Ferro TJ, Blumenstock FA, Brockenauer AM, Malik AB. (1990). Increased endothelial albumin permeability mediated by protein kinase C activation. *J Clin Invest* 85:1991–1998.

Nangaku M. (2004). Mechanisms of tubulointerstitial injury in the kidney: Final common pathways to end-stage renal failure. *Intern Med* 43:9–17.

Nicholson JK, Lindon JC, Holmes E. (1999). 'Metabonomics': Understanding the metabolic responses of living systems to pathophysiological stimuli via multivariate statistical analysis of biological NMR spectroscopic data. *Xenobiotica* 29:1181–1189.

Plumb RS, Granger JH, Stumpf CL, Johnson KA, Smith BW, Gaulitz S, Wilson ID, Castro-Perez J. (2005). A rapid screening approach to metabonomics using UPLC and oa-TOF mass spectrometry: Application to age, gender and diurnal variation in normal/Zucker obese rats and black, white and nude mice. *Analyst* 130:844–849.

Rhee SG. (2001). Regulation of phosphoinositide-specific phospholipase C. *Annu Rev Biochem* 70:281–312.

Robertson DG, Reily MD, Baker JD. (2007). Metabonomics in pharmaceutical discovery and development. *J Proteome Res* 6:526–539.

Wenk MR. (2005). The emerging field of lipidomics. *Nat Rev Drug Discov* 4:594–610.

Wilson ID, Nicholson JK, Castro-Perez J, Granger JH, Johnson KA, Smith BW, Plumb RS. (2005). High resolution "ultra performance" liquid chromatography coupled to oa-TOF mass spectrometry as a tool for differential metabolic pathway profiling in functional genomic studies. *J Proteome Res* 4:591–598.

Wolf G. (2006). Renal injury due to renin-angiotensin-aldosterone system activation of the transforming growth factor-beta pathway. *Kidney Int* 70:1914–1919.

Yang J, Zhao X, Liu X, Wang C, Gao P, Wang J, Li L, Gu J, Yang S, Xu G. (2006). High performance liquid chromatography-mass spectrometry for metabonomics: Potential biomarkers for acute deterioration of liver function in chronic hepatitis B. *J Proteome Res* 5:554–561.

Yin P, Zhao X, Li Q, Wang J, Li J, Xu G. (2006). Metabonomics study of intestinal fistulas based on ultraperformance liquid chromatography coupled with Q-TOF mass spectrometry (UPLC/Q-TOF MS). *J Proteome Res* 5:2135–2143.

Yokozawa T, Zheng PD, Oura H, Koizumi F. (1986). Animal model of adenine-induced chronic renal failure in rats. *Nephron* 44:230–234.

Yu HT. (2003). Progression of chronic renal failure. *Arch Intern Med* 163:1417–1429.

Zoccali C. (2006). Traditional and emerging cardiovascular and renal risk factors: An epidemiologic perspective. *Kidney Int* 70:26–33.